Check for updates

Adsorption of gas molecules on a graphitic GaN sheet and its implications for molecule sensors

Yongliang Yong, [ID] *[a] Hongling Cui,[a] Qingxiao Zhou,[a] Xiangying Su,[a] Yanmin Kuang[b] and Xiaohong Li[a]

Motivated by the recent realization of two-dimensional (2D) nanomaterials as gas sensors, we have investigated the adsorption of gas molecules (SO_2, NO_2, HCN, NH_3, H_2S, CO, NO, O_2, H_2, CO_2, and H_2O) on the graphitic GaN sheet (PL-GaN) using density functional theory calculations. It is found that among these gases, only SO_2 and NH_3 gas molecules are chemisorbed on the PL-GaN sheet with apparent charge transfer and reasonable adsorption energies. The electronic properties (especially the electric conductivity) of the PL-GaN sheet showed dramatic changes after the adsorption of NH_3 and SO_2 molecules. However, the strong adsorption of SO_2 on the PL-GaN sheet makes desorption difficult, which precludes its application to SO_2 sensors. Therefore, the PL-GaN sheet should be a highly sensitive and selective NH_3 sensor with short recovery time. Furthermore, the adsorption of NO (or NO_2) molecules introduces spin polarization in the PL-GaN sheet with a magnetic moment of about 1 μ_B, indicating that magnetic properties of the PL-GaN sheet are changed obviously. Based on the change of magnetic properties of the PL-GaN sheet before and after molecule adsorption, the PL-GaN sheet could be used as a highly selective magnetic gas sensor for NO and NO_2 detection.

1. Introduction

Two-dimensional (2D) nanomaterials, such as silicene[1–4] and phosphorene,[5–7] have become prominent in gas sensor applications in recent years.[8] This is because a new generation of gas sensors has been developed using graphene due to its excellent properties such as high sensitivity to detect various gas molecules, large sensing area per unit volume, low electronic temperature noise, fast response time, and high chemical stability.[9,10] The 2D nanomaterials have a large surface-to-volume ratio and a large associated charge transfer between gas molecules and the substrates.

Due to their outstanding electronic properties, gallium nitride (GaN) nanomaterials are usually good candidates for gas sensors.[11–18] For example, in two recent studies, we have demonstrated theoretically that $Ga_{12}N_{12}$ nanoclusters are potentially good NO, NO_2, and HCN gas sensors,[16] and cluster-assembled nanowires based on the $Ga_{12}N_{12}$ cluster can be an appropriate gas sensor for CO, NO, and NO_2 detection.[17] However, as we know, the investigation of 2D GaN as gas sensors has not been reported. In recent years, a large number of 2D semiconductor materials in the group III–V family are identified since 2D materials present a whole new class of

materials whose properties differ from those of their three-dimensional (3D) counterparts and hold great promise in nanodevice applications.[19–28] Among the 2D semiconductor materials, 2D gallium nitride (GaN) has been investigated theoretically[19–25] and experimentally.[26–28] It would be interesting and is important to continue studying the feasibility of 2D GaN as gas sensors considering the promising applications of GaN and 2D nanomaterials in gas sensors.

Monolayer graphitic GaN sheet with an atomically flat planar honeycomb hexagonal structure (named as PL-GaN) was predicted theoretically to be stable.[21–23] The structure of PL-GaN is similar to that of graphene. For the investigation of graphene as gas sensor,[9,10] it is shown that the charge carrier concentration induced by gas molecule adsorption can be used to make highly sensitive sensors, even detecting an individual molecule, where the sensor properties are based on changes in the resistivity with the gas molecules acting as donors or acceptors. It is expected that the electrical resistivity of the PL-GaN sheet will also be influenced by the gas molecule adsorption in a similar way. In the present work, we employ first-principles calculations to accurately describe the adsorption behavior and electronic properties of the SO_2, NO_2, HCN, NH_3, H_2S, CO, NO, O_2, H_2, CO_2, and H_2O molecules on the PL-GaN sheet, in order to explore the feasibility of using the PL-GaN sheet as reusable gas sensors. It is well known that pollutional components, such as SO_2, NO_2, HCN, NH_3, H_2S, CO, and NO are the byproduct of various chemical and biological processes and considered to be hazardous, more importantly, they are the most common

[a]College of Physics and Engineering, Henan University of Science and Technology, Luoyang 471023, People's Republic of China. E-mail: ylyong@haust.edu.cn; Tel: +86 187 36385204

[b]Institute of Photobiophysics, School of Physics and Electronics, Henan University, Kaifeng 475004, People's Republic of China

pollutional gases in industrial and agricultural production, and our daily life. To have a compare with the normal gases, we also considered the gases such as O_2, H_2, CO_2, and H_2O. Our results showed that NH_3 and SO_2 were preferably chemically adsorbed on the PL-GaN sheet with reasonable adsorption energies and apparent charge transfers between the molecules and the PL-GaN sheet. Other molecules were prone to physically adsorbing on the PL-GaN sheet. Apparently, the band structures were modified after adsorption of NH_3 and SO_2 molecules, indicating that the adsorption of the two molecules changed the electronic properties of the PL-GaN sheet. Considering the recovery time, the PL-GaN sheet should be a promising gas sensor for NH_3 detection. On the other hand, based on a new transduction principle, which is the exploitation of magnetic instead of electrical properties modifications due to surface–gas interaction in the active material, the PL-GaN sheet can be exploited as a highly selective magnetic gas sensor for NO and NO_2 detection.

2. Computational methods

In our study, all calculations were performed using the spin-polarized density functional theory (DFT) that was implemented in the DMol^3 package.[29,30] The generalized gradient approximation in the Perdew, Burke, and Ernzerhof (PBE)[31] form with van der Waals (vdW) correction, as proposed by Tkatchenko and Scheffler (TS method),[32] was chosen to describe the exchange–correlation energy function. The double numerical basic sets that were supplemented with d polarization functions (*i.e.* the DNP set) and all-electron core treatment were selected. The convergence criterion was set to 10^{-6} a.u. for energy and electron density in the self-consistent field calculations. The geometries were fully optimized without any constraints for symmetry. The convergence criterion of 10^{-3} a.u. for the gradient and displacement and 10^{-5} a.u. for the total energy in geometrical optimization were used. The Brillouin zone was sampled by $10 \times 10 \times 1$ special k-points in the Monkhorst–Pack scheme.[33] To prevent interactions between the adjacent supercells a minimum of 20 Å vacuum space is kept.

In order to evaluate the stability of molecules adsorption on the PL-GaN sheet, the adsorption energy (E_{ads}) is defined as $E_{ads} = E_{(gas-GaN)} - E_{(GaN)} - E_{(gas)}$, where $E_{(gas-GaN)}$, $E_{(GaN)}$ and $E_{(gas)}$ represent the total energy with full relaxation for the gas molecule adsorbed on the PL-GaN sheet, the corresponding pristine PL-GaN sheet and single gas molecule, respectively. With such a definition, negative adsorption energy indicated that the adsorption was exothermic. The charge transfer between PL-GaN and the absorbed molecules was analyzed with Hirshfeld's analysis.[34] The accuracy of the GGA-PBE and DNP combination to be used in investigations of the structural and electronic properties of (gases adsorption on) GaN systems has been demonstrated.[16,17,35–37]

3. Results and discussion

3.1 The geometry and stability of the PL-GaN sheet

To model the monolayer graphitic GaN sheet (PL-GaN), we used a 4×4 supercell, as shown in Fig. 1(a), which has a lattice

dimensions of 12.955×12.955 Å corresponding to the optimized lattice parameter of $a = 3.239$ Å, which is in good agreement with previous reports.[21–23] To assess the feasibility of using a PL-GaN sheet as a gas sensor, we needed to carefully consider if it could be used in an experimental environment to enable effective characterization and application. In this context, a first-principles Born–Oppenheimer molecular dynamics (BOMD) simulation within a NVT ensemble was carried out for the structure of the PL-GaN sheet, to examine its dynamic behavior and thermal stability. We used a Nosé–Hoover chain of thermostats to influence the temperature. The GGA-PBE and DNP combination was used for BOMD. Our simulation time was set at 4 ps with a time step of 1 fs. We used a constant average temperature of 300 K when the trajectories were calculated. How the total energy of the structure varied during the simulation is shown in Fig. 1(b). After 4 ps, we observed no destruction of the structure of the PL-GaN sheet. Furthermore, Fig. 1(b) shows that the energy of the PL-GaN oscillated around the same energy value for the duration of the simulation (the range of energy vibration was no more than 0.01 eV). This fact does indeed support the thermal stability of the structure that was calculated. We found, *via* these results, that the structure of our PL-GaN sheet was in fact stable at room temperature, and it was stable for a long enough period of time to enable its characterizations and applications.

3.2 The adsorption of molecular gases on the PL-GaN sheet

Firstly, the adsorption behaviors of various gas molecules (including SO_2, NO_2, HCN, NH_3, H_2S, CO, NO, O_2, H_2, CO_2, and H_2O) on the PL-GaN sheet have been investigated. We set up many initial structures for each molecule adsorbed on the PL-GaN sheet to obtain the most stable structures of the molecule-sheet systems. For the PL-GaN sheet, four possible starting adsorption sites have been considered, namely, two tops (Ga and N atom), hollow and bridge sites. Meanwhile, for each adsorption site, we also examined different molecular orientations. For example, for diatomic gases (CO or NO), we considered three possible orientations. The molecule axis was oriented parallel or perpendicular (with the O atom pointing up or down) with respect to the PL-GaN sheet. Each initial structure was fully relaxed. The most stable configurations of each molecular gas adsorbed on the PL-GaN sheet were presented in Fig. 2 and 4, and the calculated adsorption energy (E_{ads}), charge transfer (E_T), adsorption distances (D) between the adsorbed molecule and the PL-GaN sheet, and the band energy gap (E_g) were summarized in Table 1.

Then, we investigate the adsorption of SO_2 molecule on the PL-GaN sheet. As shown in Fig. 2(a), for the most stable configuration of SO_2 molecule adsorption on the PL-GaN sheet, it was observed that the SO_2 molecule prefers to adopt the orientation of O–S–O parallel to one edge of Ga–N–Ga in the PL-GaN sheet. From Table 1, one can see that SO_2 has the largest E_{ads} of -1.060 eV among the gas molecules studied in the present work. There are two stable chemical O–Ga bond length of 2.06 Å and one stable chemical S–N bond length of 1.79 Å, which indicates that the SO_2 molecule is chemisorbed on the
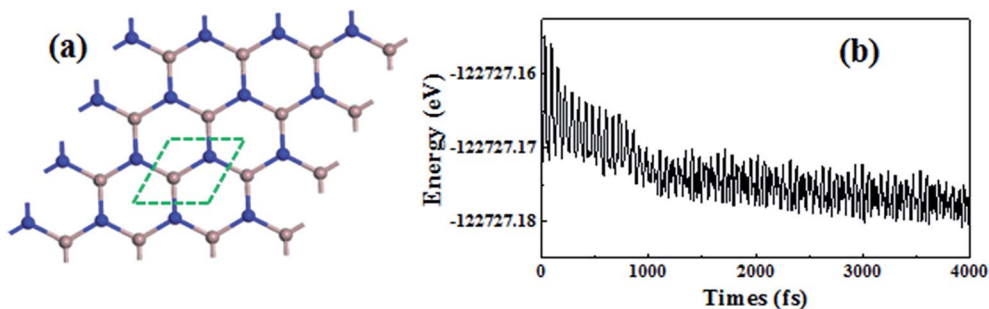
Fig. 1 (a) The structure of the PL-GaN sheet. The range around by green dashed line marks the primitive unit cell for the corresponding sheet. Ga and N atoms are brown and blue, respectively. (b) Total energy (eV) *versus* time ($T = 300$ K) for the structure of the PL-GaN sheet.
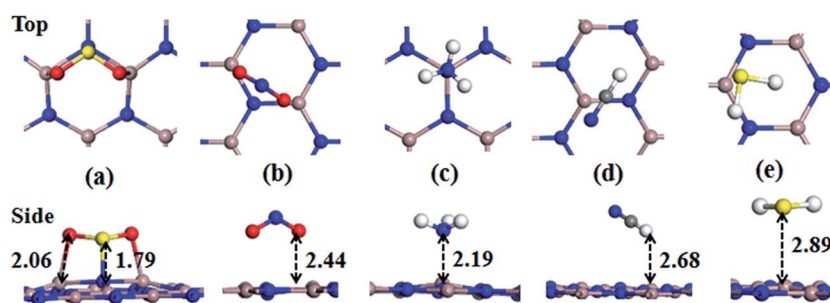

Fig. 2 The top and side views for the most stable structures of the PL-GaN sheet with gas molecule adsorption: (a) SO_2; (b) NO_2; (c) NH_3; (d) HCN; (e) H_2S. Only the structure around the adsorbed molecule is shown in figure. The adsorption distances (in Å) between the molecule and the PL-GaN sheet are also given. S, O, C and H atoms are yellow, red, grey and white, respectively.

PL-GaN sheet. Because of the adsorption of SO_2 molecule on PL-GaN sheet, a charge transfer of $0.209e$ ($e = -1.6 \times 10^{-19}$ C) from the SO_2 molecule to the PL-GaN sheet is found. Although the structure of NO_2 molecule is similar to that of SO_2, the adsorption behavior of NO_2 on PL-GaN sheet is very different from that of SO_2 on the PL-GaN sheet. The most stable configuration of NO_2 on the PL-GaN sheet is shown in Fig. 2(b). Our

result shows that the NO_2 molecule is physically adsorbed on the PL-GaN sheet with the shortest distance between NO_2 molecule and the PL-GaN sheet of 2.44 Å. This is very different from the cases of NO_2 molecule adsorbed on GaN nanotube,[15] nanocluster[16] and nanowires.[17] Khan *et al.*,[15] for example have investigated the interactions between armchair (4,4)GaN nanotube and NO_2 toxic gas molecules. They found that the NO_2

Table 1 The calculated adsorption energy (E_{ads}), charge transfer, adsorption distances (D) between the adsorbed molecule and the PL-GaN sheet, the band energy gap (E_g), the electrical conductivity (σ, which is calculated by using $\sigma \propto \exp\left(\dfrac{-E_g}{2kT}\right)$), and the recovery time (Re) for the most stable configurations of each molecule adsorption on the PL-GaN sheet

System[a]	E_{ads} (eV)	$E_T{}^b$ (e)	D^c (Å)	E_g (eV)	σ	Re (s)
SO_2/PL-GaN	−1.060	−0.209	Ga–O: 2.06, S–N: 1.79	2.729	1.6×10^{-23}	4.3×10^5
NO_2/PL-GaN	−0.493	−0.081	2.44	0.388	5.7×10^{-4}	1.6×10^{-4}
HCN/PL-GaN	−0.300	−0.028	2.68	2.637	9.5×10^{-23}	9.8×10^{-8}
NH_3/PL-GaN	−0.871	0.231	2.19	2.583	2.7×10^{-22}	3.1×10^2
H_2S/PL-GaN	−0.446	0.139	2.89	2.636	9.7×10^{-23}	2.6×10^{-5}
CO/PL-GaN	−0.263	0.047	2.71	2.644	8.3×10^{-23}	2.4×10^{-8}
NO/PL-GaN	−0.364	0.004	2.48	0.670	2.5×10^{-6}	1.1×10^{-6}
O_2/PL-GaN	0.198	−0.011	2.99	0.589	1.2×10^{-5}	5.1×10^{-16}
H_2/PL-GaN	−0.150	−0.021	2.85	2.640	8.9×10^{-23}	3.1×10^{-10}
CO_2/PL-GaN	−0.259	0.017	3.28	2.631	1.1×10^{-22}	2.0×10^{-8}
H_2O/PL-GaN	−0.591	0.092	2.30	2.606	1.7×10^{-22}	6.8×10^{-3}

[a] Notations: *e.g.* SO_2/PL-GaN represents the most stable adsorption configuration of SO_2 on the PL-GaN sheet. [b] Positive value means the charge transfer from the PL-GaN to molecules, whereas the negative value is opposite. [c] Adsorption distance (D) is defined as the shortest atom-to-sheet distance between the molecule and the PL-GaN sheet.

molecule is chemically adsorbed on the GaN nanotube surface with apparent E_{ads} of −0.99 eV and an adsorbate distance of 1.94 Å. Likewise, the adsorption behavior of NO_2 molecule on GaN nanocluster[16] and nanowires[17] is chemisorption with obvious E_{ads} and strong charge transfer. However, the adsorption of NO_2 molecule on the PL-GaN sheet results in E_{ads} of −0.493 eV, and the charge transfer between the molecule and sheet is only 0.081e.

For the NH_3 molecule adsorption on the PL-GaN sheet, it is found that the N atom in NH_3 is directly bonded to one Ga atom in the PL-GaN sheet with relatively large E_{ads} of −0.871 eV, very similar to the cases of NH_3 molecule adsorbed on GaN nanotube,[15] transition metal-doped graphene[38,39] or carbon nanotubes.[40] Meanwhile, the corresponding adsorbate distance of Ga–N bond between the N atom in NH_3 and the Ga atom in sheet is 2.19 Å, which is a little larger than the Ga–N bond lengths in the PL-GaN sheet, but similar to the Ga–N bond lengths in the small GaN clusters[36,37,41–43] and nonpolar GaN surface.[44] These results indicate that NH_3 molecule is chemisorbed on the PL-GaN sheet. Furthermore, a charge transfer of 0.231e from the molecule to the PL-GaN sheet is observed due to the adsorption of NH_3 molecule. In recent years, adsorption of NH_3 on GaN (0001) surface with mixed ambients have been theoretically investigated by Krukowski group.[45–47] They found that the NH_3 adsorbed molecularly on the GaN surface is in a metastable state, thus NH_3 adsorption is dissociative and leads to decomposition of NH_3 to H and NH_2 radical, indicating that the dissociative adsorption of NH_3 is favorable energetically. To investigate the dissociation of NH_3 on the PL-GaN surface, we investigated the reaction of NH_3 to H and NH_2 on the PL-GaN surface, whose pathway can be written as $NH_3 \rightarrow$ H + NH_2. Transition state (TS) geometries were first searched by the linear/quadratic synchronous transit (LST/QST) methods and then fully optimized. As the product and reactant, we only considered the most stable configurations of NH_3 and NH_2 + H on the PL-GaN surface. After relaxing the initial structures of H + NH_2 on the PL-GaN surface, we obtained its most stable configuration, which is shown in Fig. 3 as named as NH_2 + H/ PL-GaN. The NH_2 is bonded with a Ga atom within a Ga–N

bond length of 1.907 Å, while the H atom is bonded with an adjacent N atom with a H–N bond length of 1.048 Å. Then, we considered the reaction path of the chemisorption configuration of NH_2 + H on the PL-GaN surface. The calculated results are depicted in Fig. 3. As shown in Fig. 3, the NH_2 + H product is formed through a transition state (*i.e.* TS, TS has only one imaginary frequency of 1248.9i cm^{-1}). In TS the distance between the N atom in NH_2 and the single H atom is 1.385 Å, much larger than that of N–H distances in NH_3 and NH_2. To form the NH_2 + H product from NH_3, an energy barrier of about 0.868 eV must overcome, and the reaction is endothermic with binding energy of 0.601 eV. Conversely, the reaction from the NH_2 + H/PL-GaN configuration to the NH_3/PL-GaN configuration only has to overcome a small energy barrier of 0.279 eV with moderate binding energy of −0.601 eV. This reaction path clearly indicates that for NH_3 molecule adsorbed on the PL-GaN surface, the dissociation of NH_3 molecule to a NH_2 radical and a H adatom is much less favorable. This is very different from that of NH_3 on GaN (0001) surface.[45–47]

The most stable configurations of HCN, H_2S, CO, NO, O_2, H_2, CO_2, and H_2O molecular gases adsorbed on the PL-GaN sheet were shown in Fig. 2 and 4, and the corresponding calculated results were listed in Table 1. Although we have considered all possible initial structures of these molecular gases on the PL-GaN sheet, these molecules are energetically favorable to physically adsorb on the PL-GaN sheet with inconspicuous charge transfer. Particularly, the adsorption of O_2 molecule on the PL-GaN sheet is endothermic, indicating that the PL-GaN sheet is very inert to oxidation, similar to that of O_2 adsorption on GaN nanowires.[17] The adsorption of H_2 molecule on the PL-GaN surface is very different from the adsorption of hydrogen at the GaN surface.[48,49] Krukowski group[48,49] has found that for relatively low hydrogen coverage, the H_2 molecule adsorbs dissociatively, leading to disintegrating into separate H atoms at GaN (0001) surface.

In general, the adsorption energies can reveal the strong or weak interaction between the molecule and the PL-GaN sheet. To gain more insight into the stability of molecular gases adsorbed on the sheet, we then investigated the change of the electronic structure of the PL-GaN sheet with gas molecules adsorption. The density of states (DOS) and electronic band structures were studied for the most stable structures of each molecule adsorbed on the PL-GaN sheet. All the calculated band gaps were listed in Table 1, and all band structures and only some selected DOSs of the most stable adsorption configurations were shown in Fig. 5 and 6, respectively. A indirect gap of 2.632 eV is found for the PL-GaN sheet, which is smaller than the results obtained from HSE06 calculations.[21] This is mainly because that our calculations are not considered the hybrid functional. It is noting that our focus is mainly concerned on the change of band gap. As discussed in a previous section, only the NH_3 and SO_2 molecules were chemisorbed on the PL-GaN sheet, accompanied by an apparent charge transfer. Accordingly, the band structures in the PL-GaN sheet were modified apparently after the SO_2 and NH_3 molecule adsorption compared with the band structure of the pure PL-GaN sheet, indicating that the electronic properties of the PL-GaN sheet are
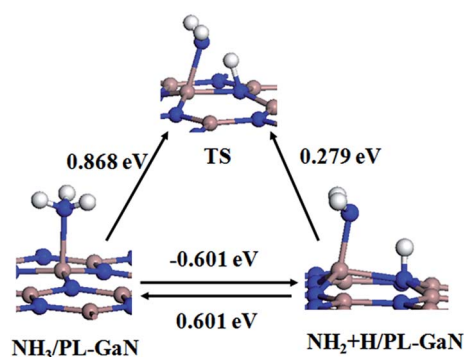

Fig. 3 Reaction path from the chemisorption structure of NH_3 on the PL-GaN surface (named as NH_3/PL-GaN) to the structure of NH_2 radical and H adatom on the PL-GaN surface (named as NH_2 + H/PL-GaN).
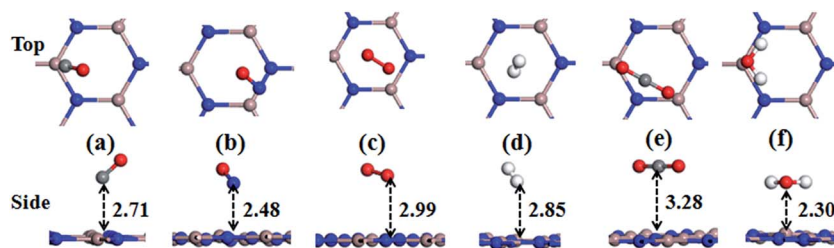
Fig. 4 The top and side views for the most stable structures of PL-GaN sheet with gas molecule adsorption: (a) CO; (b) NO; (c) O_2; (d) H_2; (e) CO_2; (f) H_2O. Only the structure around the adsorbed molecule is shown in figure. The adsorption distances (in Å) between the molecule and the PL-GaN sheet are also given.

changed by the NH_3 and SO_2 molecules adsorption. Furthermore, comparing with the DOS of the pure PL-GaN sheet, the total DOSs of the molecule–sheet compositions and LDOS of the corresponding molecules show that the considered molecular gases modulate the electronic properties of the PL-GaN sheet in different ways: (i) the chemical adsorption of SO_2 and NH_3 molecules introduces unoccupied local states in the conduction band, suggesting that the conductance of these systems can be enhanced notably. Also, LDOS analysis showed that adsorption of NH_3 and SO_2 molecules produced fully occupied states in the valence band, and these states were nonlocalized, indicating

that the interaction between these molecules and the sheet was strong. This was consistent with the calculated adsorption energy. (ii) LDOS analysis indicated that NO_2 adsorption introduced certain impurity states in the band gap and localized states near the Fermi level were created, thus adsorption of NO_2 decreased the original band gap. (iii) Impurity states in the band gap were also introduced by NO molecule adsorption, while the Fermi level of this system crossed these states. Thus, similar to the case of NO_2 adsorption, the adsorption of NO decreased the original band gap. (iv) Taking the case of H_2S adsorption as an example, from the LDOS analysis we can see
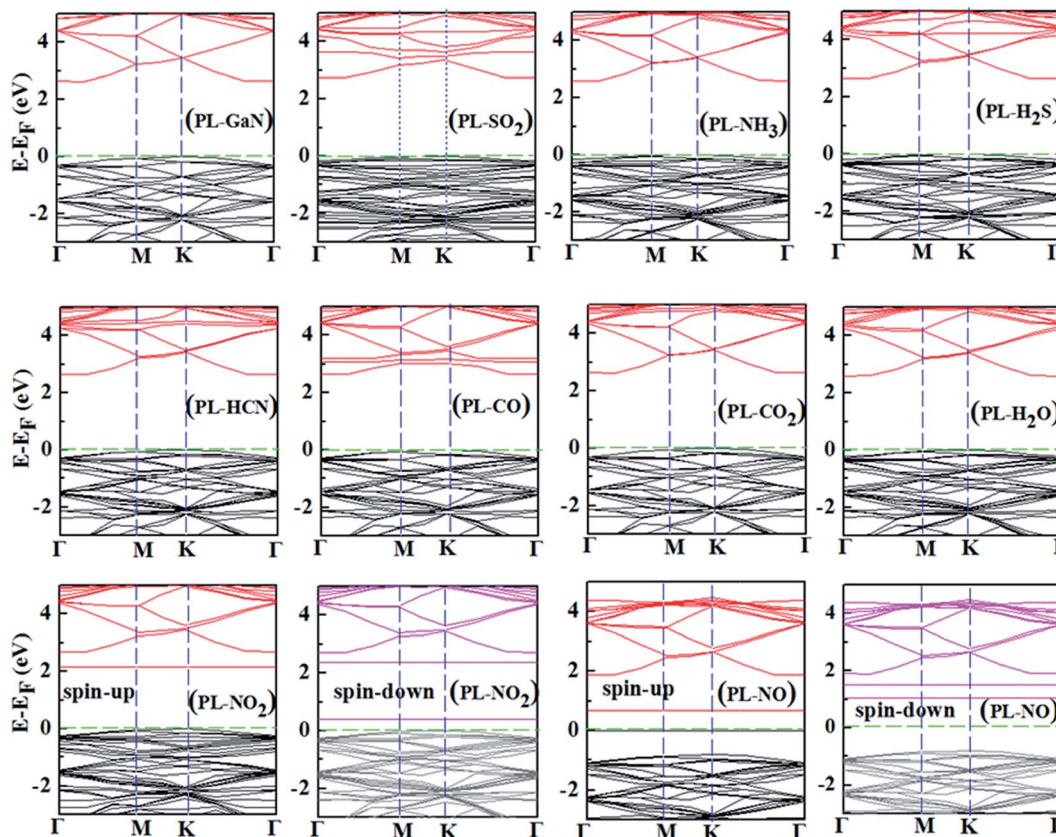

Fig. 5 The band structures for the most stable structures of SO_2, NH_3, H_2S, HCN, CO, CO_2, H_2O, NO_2 and NO adsorption on the PL-GaN sheet. The Fermi-level energy was set to zero and is marked by green dotted lines. As a note of this figure, for example, the configuration of SO_2 on the PL-GaN sheet is marked as "PL-SO_2". Due to the introduction of spin polarization for NO_2 and NO adsorption, the spin-up and spin-down bands are shown, while the others are only shown with spin-up bands.
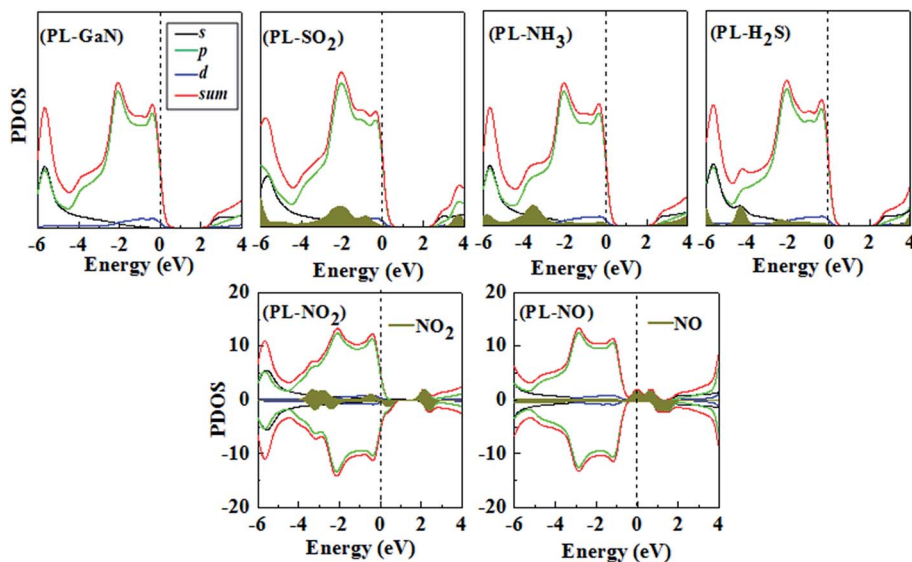
Fig. 6 Total and partial density of states (DOS) of the most stable structures of the PL-GaN sheet and its adsorption systems with SO_2, NH_3, H_2S, NO_2, and NO. The Fermi-level energy is marked by vertical dashed line. The LDOS of gas molecules is also plotted (dark yellow filled area under the DOS curve). The positive and negative values represent spin-up and spin-down states, respectively.

that the states contributed by H_2S molecule are located around the valence band indicating the conductance of this system cannot be changed.

3.3 The possibility of the PL-GaN as a gas sensor

In general, a good commercial sensor should face the following challenges: sensor sensitivity, selectivity, stability, and speed (response and recovery rate), namely the "4s". Next, we would discuss the possibility of the PL-GaN as a gas sensor for some certain gas detection, that is, whether the gas sensors based on PL-GaN can exhibit better performances.

If the PL-GaN sheet is indeed effective as a gas sensor for certain gas detection, the molecular gases would be chemically adsorbed on the PL-GaN sheet with apparent E_{ads}. In addition, there will be sufficient charge transfer with the PL-GaN sheet to affect the electrical conductivity of the PL-GaN sheet. As mentioned above, the PL-GaN sheet is particularly stable at room temperature. After the molecules adsorption, it is found that there is no structural deformation in PL-GaN sheet, further indicating that the stability of the PL-GaN sheet. It can be seen from Table 1 that the E_{ads} of SO_2 and NH_3 molecules on the PL-GaN sheet is much larger than that of other molecules on the sheet, indicating the strong interaction between the (SO_2 or NH_3) molecules and the PL-GaN sheet. Meanwhile, these large adsorption energies can prevent spontaneous desorption at room temperature. Particularly, the SO_2 and NH_3 molecules are chemisorbed on the sheet. These results show that the adsorption of SO_2 and NH_3 exhibits more stability than the cases of other molecules. More importantly, because of the adsorption of SO_2 (NH_3), there are apparent charge transfers (more than $0.2e$) between the SO_2 (NH_3) molecule and the PL-GaN sheet. However, the other considered molecules only prefer to physically adsorb on the PL-GaN sheet with small E_{ads}

and few charge transfer. These results indicate that the PL-GaN sheet is highly sensitive and selective to the adsorption of SO_2 (NH_3) molecule.

In addition, we used the following equation to estimate the electric conductivity change of the PL-GaN sheet before and after adsorption:[50]

$$\sigma \propto \exp\left(\frac{-E_g}{2kT}\right),$$

where σ is the electric conductivity of the configurations, E_g is the band gap value of the configurations, k is the Boltzmann's constant, and T is the thermodynamic temperature. We found that the change of band gaps for the most stable structures of NH_3 and SO_2 molecules adsorbed on the PL-GaN sheet was 0.097 and 0.049 eV with respect to the corresponding pure sheet. Therefore, the NH_3 and SO_2 molecules can be detected by calculating the conductivity change in the PL-GaN sheet before and after the adsorption process. However, the band gap energies of the PL-GaN sheet are barely influenced by the physical adsorption of other molecules (except for NO and NO_2, which would be discussed individually later in this article). This shows that the conductivity changes for SO_2 and NH_3 molecules are much larger than that of HCN, H_2S, CO, H_2, CO_2, and H_2O, further indicating the high sensitivity and selectivity of the PL-GaN sheet as a gas sensor for SO_2 and NH_3 detection. To further intuitively illustrate these results, we calculated the electric conductivity (σ) by using the above mentioned formula, in which we assume the temperature is at 300 K. All results are listed in Table 1. The electric conductivity of the pure PL-GaN sheet at 300 K is calculated to be 1.0×10^{-22}. From Table 1, it is found that the conductivity for SO_2 and NH_3 molecules adsorption is about 10 and 2 times, respectively, compared with that of the pure PL-GaN sheet. For NO and NO_2 adsorption, the changes of conductivity are much larger.

It is worth noting, however, that strong adsorption of a certain molecule on the PL-GaN sheet implies that desorption of this gas molecule from the PL-GaN sheet could be quite complicated; the device may require a long recovery time. The transition state theory gives the relation between the recovery time (τ) and the adsorption energy (E_{ads}) as follows:

$$\tau = \nu_0^{-1} e^{-E_{ads}/kT},$$

where ν_0 is the attempt frequency, k is the Boltzmann's constant, and T is the temperature. Using the formula, Peng et al.[51] predicted that for carbon nanotube-based NO_2 sensor the recovery time at room temperature is in the range of 5 μs to 16 s, which corresponds to the adsorption energy range of −0.34 to −0.79 eV, particularly, the 12 hour recovery time relates to an E_{ads} of −1.00 eV. Supposing all we considered molecules have the same order of magnitude for the attempt frequency as NO_2 ($\nu_0 = 10^{12}$ s^{-1}), we can estimate the recovery time of all considered molecules at $T = 300$ K. The results are listed in Table 1. The strong adsorption energy (−1.060 eV) of SO_2 molecule on the PL-GaN sheet would match a recovery time of 4.3×10^5 s, much more than 12 hours, which precludes the applications of the PL-GaN sheet as a reusable sensor for SO_2 gas, but it can be used as a disposable gas sensor for SO_2 gas. However, the adsorption energy of NH_3 molecule on the PL-GaN sheet is moderate (−0.871 eV), which corresponds to a short recovery time of about 5.2 minutes for the PL-GaN sensor for NH_3 detection at room temperature. The recovery times of others are much shorter. For example, the recovery time of NO and NO_2 is 1.1×10^{-6} s and 1.6×10^{-4} s, respectively.

Based on analyzing adsorption energies, forms of adsorption (chemically or physically), charge transfer, and the change of band structures, the PL-GaN sheet exhibits strong sensitivity and selectivity for SO_2 and NH_3, while it appears inefficient to sense HCN, H_2S, CO, O_2, H_2, CO_2, and H_2O. In combination with the fact that the recovery time, the PL-GaN sheet should be a promising reusable sensor for highly sensitive and selective NH_3 detection with short recovery time, and a disposable sensor for SO_2 detection.

Because of the physisorption of NO (or NO_2) on the PL-GaN sheet, the adsorption energies are smaller and few electrons transferred between the molecule and the sheet, which suggest that the interaction between NO (or NO_2) and the PL-GaN sheet is weak. Based on these results, it can be concluded that the PL-GaN sheet is not suitable for sensing NO and NO_2. However, it should be noted that the above analysis of the PL-GaN sheet as gas sensing materials is based on their semiconducting properties, that is to say, the transduction principle is the exploitation of electrical properties modifications due to the sheet–gas interaction.

In recent years, there is a completely new transduction principle, which is the exploitation of magnetic instead of electrical properties modifications due to surface–gas interaction in the active material.[52–56] That is to say, analyzing change in magnetic properties of substrates upon interaction with gases could be a new way to detect gases. For example, Matatagui et al.[55,56] reported the combination of a magnetostatic surface wave oscillator with a layer of magnetic oxide

nanoparticles in what they called a magnonic gas sensor. The perturbation of the magnetic properties of the magnetic oxide layer induces a frequency shift in the magnetostatic surface wave oscillator that can be registered in the presence of different gases. The pure PL-GaN sheet is non-magnetic. The adsorption of NO (or NO_2) molecule introduces spin polarization in the PL-GaN sheet, which has a magnetic moment of about 1 μ_B, indicating that magnetic properties of the PL-GaN sheet is changed obviously due to the adsorption of NO (or NO_2) molecule, which is similar to the cases of NO (or NO_2) on $Ga_{12}N_{12}$ nanocluster[16] and nanowires.[17] However, the net spin polarization of the PL-GaN sheet is not modified due to the adsorption of other molecules. In this regard of the change of magnetic properties, the PL-GaN sheet is highly selective. Analyzing the change in magnetic properties of the PL-GaN sheet upon interaction with NO (or NO_2) gas could be a new strategy for detecting NO (or NO_2) using the PL-GaN sheet as gas sensors. The adsorption energies of NO (or NO_2) on the PL-GaN sheet is small, but it suggests that the recovery time would be very short. Therefore, the PL-GaN sheet could be used as a highly selective magnetic gas sensor for NO and NO_2 detection with short recovery time.

4. Conclusions

In conclusion, using first-principled calculations based on density functional theory, the adsorption of gas molecules (SO_2, NO_2, HCN, NH_3, H_2S, CO, NO, O_2, H_2, CO_2, and H_2O) on the graphitic GaN sheet with an atomically flat planar honeycomb hexagonal structure (PL-GaN) have been investigated. We have obtained the adsorption geometries, adsorption energies, charge transfer, and electronic properties of each molecule on the PL-GaN sheet. It is found that among these gases, only SO_2 and NH_3 gas molecules are chemisorbed on the PL-GaN sheet. After the adsorption of SO_2 and NH_3 molecules, the electronic properties of the PL-GaN sheet present dramatic changes, especially regarding their electric conductivity. Other gas molecules prefer to physically adsorb on the PL-GaN sheet, and these adsorptions hardly change the electronic properties of the PL-GaN sheet. However, the very strong adsorption of SO_2 on the PL-GaN sheet makes desorption difficult, which precludes its applications to SO_2 sensors. Due to the short recovery time, reasonable adsorption energies, the change of the electric conductivity, and the apparent charge transfer, the PL-GaN sheet should be a good NH_3 sensor with quick responses as well as short recovery times.

The pure PL-GaN sheet is non-magnetic. However, we found that the adsorption of NO (or NO_2) molecule introduces spin polarization in the PL-GaN sheet, which corresponds to a magnetic moment of approximately 1 μ_B, indicating that magnetic properties of the PL-GaN sheet is changed obviously due to the adsorption of NO (or NO_2) molecule. Based on the transduction principle, which is the exploitation of magnetic instead of electrical properties modifications due to surface–gas interaction in the active material, the PL-GaN sheet can be used as a highly selective magnetic gas sensor for NO and NO_2 detection with short recovery time.

Conflicts of interest

There are no conflicts to declare.

Acknowledgements

References

1 W. Hu, N. Xia, X. Wu, Z. Li and J. Yang, *Phys. Chem. Chem. Phys.*, 2014, **16**, 6957–6962.

2 J. Prasongkit, R. G. Amorim, S. Chakraborty, R. Ahuja, R. H. Scheicher and V. Amornkitbamrung, *J. Phys. Chem. C*, 2015, **119**, 16934–16940.

3 T. Hussain, T. Kaewmaraya, S. Chakraborty and R. Ahuja, *J. Phys. Chem. C*, 2016, **120**, 25256–25262.

4 R. Chandramouli, A. Srivastava and V. Nagarjan, *Appl. Surf. Sci.*, 2015, **351**, 662–672.

5 L. Kou, T. Frauenheim and C. Chen, *J. Phys. Chem. Lett.*, 2014, **5**, 2675–2681.

6 S. Cui, H. Pu, S. A. Wells, Z. Wen, S. Mao, J. Chang, M. C. Hersam and J. Chen, *Nat. Commun.*, 2015, **6**, 8632.

7 M. Batmunkh, M. Bat-Erdene and J. G. Shapter, *Adv. Mater.*, 2016, **28**, 8586–8617.

8 S. Z. Butler, S. M. Hollen, L. Cao, Y. Cui, J. A. Gupta, H. R. Gutiérrez, T. F. Heinz, S. S. Hong, J. Huang, A. F. Ismach, E. Johnston-Halperin, M. Kuno, V. V. Plashnitsa, R. D. Robinson, R. S. Ruoff, S. Salahuddin, J. Shan, L. Shi, M. G. Spencer, M. Terrones, W. Wind and J. E. Goldberger, *ACS Nano*, 2013, **7**, 2898–2926.

9 F. Schedin, A. K. Geim, S. V. Morozov, E. W. Hill, P. Blake, M. I. Katsnelson and K. S. Novoselov, *Nat. Mater.*, 2007, **6**, 652–655.

10 Q. He, S. Wu, Z. Yina and H. Zhang, *Chem. Sci.*, 2012, **3**, 1764–1772.

11 B. Chitara, D. J. Late, S. B. Krupanidhi and C. N. R. Rao, *Solid State Commun.*, 2010, **150**, 2053–2056.

12 S. Barth, F. Hernandez-Ramirez, J. D. Holmes and A. Romano-Rodriguez, *Prog. Mater. Sci.*, 2010, **55**, 563–627.

13 S. J. Pearton, F. Renb, Y. Wang, B. H. Chu, K. H. Chen, C. Y. Chang, W. Lim, J. Lin and D. P. Norton, *Prog. Mater. Sci.*, 2010, **55**, 1–59.

14 M. A. Abdulsattar, *Superlattices Microstruct.*, 2016, **93**, 163–170.

15 M. S. Khan and A. Srivastava, *J. Electroanal. Chem.*, 2016, **775**, 243–250.

16 H. Cui, Y. Yong, H. Jiang, L. Yang, S. Wang, G. Zhang, M. Guo and X. Li, *Mater. Res. Express*, 2017, **4**, 015009.

17 Y. Yong, H. Jiang, X. Li, S. Lv and J. Cao, *Phys. Chem. Chem. Phys.*, 2016, **18**, 21431–21441.

18 K. H. Baik, J. Kim and S. Jang, *Sens. Actuators, B*, 2017, **238**, 462–467.

19 C. L. Freeman, F. Claeyssens and N. L. Allan, *Phys. Rev. Lett.*, 2006, **96**, 066102.

20 H. Şahin, S. Cahangirov, M. Topsakal, E. Bekaroglu, E. Akturk, R. T. Senger and S. Ciraci, *Phys. Rev. B: Condens. Matter Mater. Phys.*, 2009, **80**, 155453.

21 H. L. Zhuang, A. K. Singh and R. G. Hennig, *Phys. Rev. B: Condens. Matter Mater. Phys.*, 2013, **87**, 165415.

22 A. K. Singh and R. G. Hennig, *Appl. Phys. Lett.*, 2014, **105**, 051604.

23 A. K. Singh, H. L. Zhuang and R. G. Hennig, *Phys. Rev. B: Condens. Matter Mater. Phys.*, 2014, **89**, 245431.

24 F. Ersan, E. Aktürk and S. Ciraci, *Phys. Rev. B*, 2016, **94**, 245417.

25 H. Zhang, F. Meng and Y. Wu, *Solid State Commun.*, 2017, **250**, 18–22.

26 Z. Lin, A. Mccreary, N. Briggs, S. Subramanian, K. Zhang, Y. Sun, X. Li, N. J. Borys, H. Yuan, S. K. Fullerton-Shirey, A. Chernikov, H. Zhao, S. McDonnell, A. M. Lindenberg, K. Xiao, B. J. LeRoy, M. Drndić, J. C. M. Hwang, J. Park, M. Chhowalla, R. E. Schaak, A. Javey, M. C. Hersam, J. Robinson and M. Terrones, *2D Mater.*, 2016, **3**, 042001.

27 Z. Y. Al Balushi, K. Wang, R. K. Ghosh, R. A. Vilá, S. M. Eichfeld, J. D. Caldwell, X. Qin, Y. Lin, P. A. DeSario, G. Stone, S. Subramanian, D. F. Paul, R. M. Wallace, S. Datta, J. M. Redwing and J. A. Robinson, *Nat. Mater.*, 2016, **15**, 1166–1171.

28 N. A. Koratkar, *Nat. Mater.*, 2016, **15**, 1153–1154.

29 B. Delley, *J. Chem. Phys.*, 1990, **92**, 508–517.

30 B. Delley, *J. Chem. Phys.*, 2000, **113**, 7756–7764.

31 J. P. Perdew, K. Burke and M. Ernzerhof, *Phys. Rev. Lett.*, 1996, **77**, 3865–3868.

32 A. Tkatchenko and M. Scheffler, *Phys. Rev. Lett.*, 2009, **102**, 073005.

33 H. J. Monkhorst and J. D. Pack, *Phys. Rev. B: Solid State*, 1976, **13**, 5188–5192.

34 F. L. Hirshfeld, *Theor. Chim. Acta*, 1977, **44**, 129–138.

35 Y. Yong, B. Song and P. He, *Phys. Chem. Chem. Phys.*, 2011, **13**, 16182–16189.

36 B. Song, C. Yao and P. Cao, *Phys. Rev. B: Condens. Matter Mater. Phys.*, 2006, **74**, 035306.

37 B. Song and P. L. Cao, *Phys. Lett. A*, 2004, **328**, 364–374.

38 Y. Tang, W. Chen, C. Li, L. Pan, X. Dai and D. Ma, *Appl. Surf. Sci.*, 2015, **342**, 191–199.

39 A. S. Rad, H. Pazoki, S. Mohseni, D. Zareyee and M. Peyravi, *Chem. Phys.*, 2016, **182**, 32–38.

40 P. Buasaeng, W. Rakrai, B. Wanno and C. Tabtimsai, *Appl. Surf. Sci.*, 2017, **400**, 506–514.

41 A. Costales and R. Pandey, *J. Phys. Chem. A*, 2003, **107**, 191–197.

42 M. Zhou and L. Andrews, *J. Phys. Chem. A*, 2000, **104**, 1648–1655.

43 E. C. Perez-Angel and J. M. Seminario, *J. Phys. Chem. C*, 2011, **115**, 6467–6477.

44 L. Lymperakis and J. Neugebauer, *Phys. Rev. B: Condens. Matter Mater. Phys.*, 2009, **79**, 241308.

45 P. Kempisty, P. Strak, K. Sakowski and S. Krukowski, *J. Cryst. Growth*, 2014, **401**, 514–517.

46 P. Kempisty and S. Krukowski, *AIP Adv.*, 2014, **4**, 117109.

47 P. Kempisty, P. Strak, K. Sakowski and S. Krukowski, *J. Cryst. Growth*, 2014, **403**, 105–109.

48 P. Kempisty and S. Krukowski, *J. Cryst. Growth*, 2012, **358**, 64–74.

49 M. Ptasinska, J. Piechota and S. Krukowski, *J. Phys. Chem. C*, 2015, **119**, 11563–11569.

50 S. S. Li, *Semiconductor Physical Electronics*, Springer, USA, 2nd edn, 2006.

51 S. Peng, K. Cho, P. Qi and H. Dai, *Chem. Phys. Lett.*, 2004, **387**, 271–276.

52 A. Punnoose, K. M. Reddy, A. Thurber, J. Hays and M. H. Engelhard, *Nanotechnology*, 2007, **18**, 165502.

53 R. Ciprian, P. Torelli, A. Giglia, B. Gobaut, B. Ressel, G. Vinai, M. Stupar, A. Caretta, G. D. Ninno, T. Pincelli, B. Casarin, G. Adhikary, G. Sberveglieri, C. Baratto and M. Malvestuto, *RSC Adv.*, 2016, **6**, 83399–83405.

54 E. Comini, *Mater. Today*, 2016, **19**, 559–567.

55 D. Matatagui, O. V. Kolokoltsev, N. Qureshi, E. V. Mejía-Uriarte and J. M. Saniger, *Nanoscale*, 2015, **7**, 9607–9613.

56 D. Matatagui, O. V. Kolokoltsev, N. Qureshi, E. V. Mejía-Uriarte, C. L. Ordoñez-Romero, A. Vázquez-Olmos and J. M. Sanigera, *Sens. Actuators, B*, 2017, **240**, 497–502.